Measurement of the Proton Asymmetry Parameter in Neutron Beta Decay

M. Schumann,[1,*] M. Kreuz,[2] M. Deissenroth,[1] F. Glück,[3,4] J. Krempel,[1,†] B. Märkisch,[1] D. Mund,[1] A. Petoukhov,[2] T. Soldner,[2] and H. Abele[1,‡]

[1]*Physikalisches Institut der Universität Heidelberg, Philosophenweg 12, 69120 Heidelberg, Germany*
[2]*Institut Laue-Langevin, B.P. 156, 38042 Grenoble Cedex 9, France*
[3]*IEKP, Universität Karlsruhe (TH), Kaiserstrasse 12, 76131 Karlsruhe, Germany*
[4]*Research Institute for Nuclear and Particle Physics, POB 49, 1525 Budapest, Hungary*

(Received 14 December 2007; published 14 April 2008)

The proton asymmetry parameter C in neutron decay describes the angular correlation between neutron spin and proton momentum. In this Letter, the first measurement of this quantity is presented. The result $C = -0.2377(26)$ agrees with the standard model expectation. The coefficient C provides an additional parameter for new and improved standard model tests.

DOI: 10.1103/PhysRevLett.100.151801 PACS numbers: 13.30.Ce, 23.40.Bw, 24.80.+y

The free neutron, decaying into electron, proton, and anti-electron-neutrino (in the following called neutrino), constitutes a well suited low energy laboratory to study the structure of semileptonic weak interactions and to probe the underlying symmetries. It is a simple system without corrections due to nuclear structure. In the $V - A$ description of the standard model (SM), it is governed by two free parameters only (the Fermi constant G_F is considered to be known exactly and CP violation can be neglected): the first element of the quark mixing matrix V_{ud} and the ratio of axial-vector and vector coupling constant $\lambda = g_A/g_V$. On the other hand, there are many more experimentally accessible observables, such as the lifetime τ_n and various angular correlations between spins and momenta of the neutron and the decay products. Thus, the SM description of neutron decay is overdetermined and can be tested in many ways [1,2].

Prominent examples for angular correlation coefficients are the electron asymmetry parameter A and the neutrino asymmetry parameter B, correlating neutron spin with electron and neutrino momentum, respectively, and the correlation a between the momenta of electron and neutrino. Within the SM, each of these parameters allows to derive λ. They have been measured several times with increasing precision and are still in the focus of current research. However, the correlation between neutron spin and proton momentum, the proton asymmetry parameter, has not been determined experimentally so far. It describes the proton angular distribution [3]

$$\omega(\theta)d\cos\theta = (1 + C\cos\theta)d\cos\theta, \tag{1}$$

where we use C to label the proton asymmetry. θ is the angle between neutron spin and proton momentum. The C definition in (1) has an opposite sign compared to [3–5] to maintain the convention that a positive asymmetry indicates more particles to be emitted in spin direction. This Letter reports on the first measurements of C.

A precisely known parameter C permits new cross-checks within the SM at low energies as the three decay products are kinematically coupled,

$$C = -x_C(A + B), \tag{2}$$

where $x_C = 0.274\,84$ is a kinematical factor [3,4]. Within the SM, C gives an experimentally different access to λ (g_V and g_A are assumed to be real here):

$$C = x_C \frac{4\lambda}{1 + 3\lambda^2}, \tag{3}$$

although with somewhat smaller sensitivity than a or A. Physics beyond the SM, e.g., $V + A$-, scalar-, or tensorlike interactions, may alter this relation [4]. Thus, C is a new input parameter for global analyses of neutron decay to constrain the size of possible ''new physics'' effects. Very precise measurements of C can also provide information on recoil-order terms within the hadronic current, the weak magnetism form factor, and the Fierz interference terms b and b_ν [4–6].

A first measurement of the proton asymmetry parameter C using the electron spectrometer PERKEO II has been carried out in 2001 [7]. In the following, we report on the succeeding experiment of 2004, performed with much cleaner systematics and improved statistics.

PERKEO II was installed at the cold neutron beam position PF1B [8] of the Institut Laue-Langevin (ILL), Grenoble. Details on the experimental setup can be found in [9,10]. The neutron beam was spin polarized using two supermirror polarizers in X-SM geometry [11]. Polarization $P = 0.997(1)$ and spin-flipper efficiency $F = 1.000(1)$ were independent of position and wavelength, and stayed constant during the measurement.

PERKEO II consists of a pair of superconducting coils in split pair configuration, generating a magnetic field perpendicular to the neutron beam (cross section 50×60 mm^2), with a maximum of 1.03 T. The neutron spins align parallel to the field, that thereby divides the full solid

angle into one hemisphere in and one against spin direction. Each hemisphere was covered by an electron detector consisting of a large area plastic scintillator with photomultiplier readout. All charged decay products generated in the spectrometer center (''decay volume'') were guided onto one of the detectors by the magnetic field, realizing full $2 \times 2\pi$ coverage.

Protons were detected in coincidence with the decay electrons alike in Refs. [9,12]. The typical energies of electron and proton differ by 3 orders of magnitude. In order to detect both particles with the same detector, the protons were accelerated onto a thin (15–30 $\mu g\,cm^{-2}$) carbon foil on negative high voltage (HV). Thereby they gained enough energy to release one or several secondary electrons from the foil, which were accelerated to the plastic scintillator on ground. The decay volume itself was kept on ground potential by four grounded grids made from AlSi wires on each side. Thus all protons gained the same acceleration and the assignment of the proton to the hemisphere was not affected by the HV. The detection of the primary decay electron was not altered by the HV if the initial kinetic energy was above 84 keV, regardless of the emission angle. The energy loss of the electrons in the carbon foil was very small ($\sim$0.5 keV) and constant for all relevant electron energies, thus not leading to a systematic effect. The detection signature was an electron trigger, whose energy was recorded, followed by a proton signal. The latter arrived delayed due to the finite drift time from the decay vertex to the region of acceleration. No information on the proton energy was available with this method as the proton was detected after acceleration and as its drift time in the grounded region strongly depended on the position of the decay vertex and the emission angle relative to the magnetic field. The electron count rate was about 40 Hz for each detector, the (HV and threshold dependent) proton efficiency was up to 17%.

For each detector, we obtain four spectra, defined by particle emission in the hemisphere in (+) or against (−) neutron spin direction: $Q^{++}(E)$, $Q^{-+}(E)$, $Q^{--}(E)$, and $Q^{+-}(E)$. The first sign denotes the electron, the second the proton, and E the electron's energy. In order to derive the proton asymmetry, we have to integrate out the electron (energy and emission direction).

$$\rho^{+} = \int (Q^{++}(E) + Q^{-+}(E))dE \quad \text{and} \quad \rho^{-} = \int (Q^{+-}(E) + Q^{--}(E))dE \tag{4}$$

denote the number of protons that were emitted into one hemisphere. In this notation, the proton asymmetry parameter is given by

$$C = \frac{\rho^{+} - \rho^{-}}{\rho^{+} + \rho^{-}}. \tag{5}$$

By reversing the spin (every 2 sec) we are able to extract C from one hemisphere alone in order to avoid systematic effects from unequal proton efficiencies.

The finite electron detector threshold, the HV barrier modifying the electron detection at low energies, and electron backscattering effects prevent the evaluation of (4) in the whole energy range. Furthermore, the integrals combine events with electrons detected in two different detectors without cancellation of the related detector efficiencies. Therefore, the measured Q spectra were fitted by theoretical functions in regions high enough to describe the spectra properly where the electron detector efficiencies were 1. The spectra were then extrapolated to the full energy range and integrated, taking into account the finite detector energy resolution.

The expressions to describe the Q spectra are given in [5] with $Q^{ij} = q^{ij}F(E)$ and the Fermi function $F(E)$:

$$\begin{aligned} q^{++}_{r<1} &= \frac{2-r}{2} + \frac{a\beta}{4}\left(\frac{r^2}{2} - 1\right) + \frac{PA\beta}{2}\left(1 - \frac{2r}{3}\right) + \frac{PB}{2}\left(\frac{r^2}{3} - 1\right), \\ q^{++}_{r\geq 1} &= \frac{1}{2r}\left(1 - \frac{a\beta}{4r} + \frac{PA\beta}{3r} - \frac{2PB}{3}\right), \\ q^{--} &= q^{++}[P \rightarrow -P], \quad q^{+-} = 2 + PA\beta - q^{++}, \\ q^{-+} &= 2 - PA\beta - q^{--}, \quad \text{with} \quad r = \beta\tfrac{E+m_e}{E_{\max}-E}. \end{aligned} \tag{6}$$

A and B are the electron and the neutrino asymmetry parameter, respectively. P is the neutron beam polarization, $\beta = v/c$. $E_{\max} = 782$ keV is the end point of the beta spectrum, m_e the electron mass. Definition (6) is separated into two regions ($r < 1$, $r \geq 1$) by the energy dependent parameter r, with $r = 1$ for $E = 236$ keV.

The electron detectors were calibrated regularly using six monoenergetic conversion electron peaks (^{109}Cd, ^{139}Ce, ^{113}Sn, ^{137}Cs, and two peaks of ^{207}Bi) covering the relevant energy range up to 1 MeV. In order to correct for spatial detector effects, the decay volume projection was scanned two-dimensionally several times. Above 100 keV, detector response was linear within 0.8%. At lower energies, the linear relation $E = gk + E_{\text{off}}$ between energy E and analog-to-digital converter channel k was no longer valid. The detector gain g was known with a precision of 0.3% (0.6%) for detector 1 (detector 2). The energy offsets of the two detectors were $E_{\text{off},1} = (37.7 \pm 1.0)$ keV and $E_{\text{off},2} = (40.4 \pm 2.1)$ keV, respectively. Their uncertainty is the limiting factor for the measurement of C as it directly enters the Q^{ij} fit functions and thus alters extrapolation and integration results. It leads to an uncertainty of 0.82% on C. The uncertainties on g and the energy resolution of $\sim$15% (FWHM) at 1 MeV lead to much lower errors (0.38% and 0.12%, respectively).

A valid event consisted of an electron trigger followed by a coincident delayed proton signal. All delayed signals within a window of 82 μs were recorded for both detectors. The first 40 μs defined the coincidence window. It was chosen such that the number of protons with larger flight times was almost negligible [0.03(1)% correction on

C]. Accidental coincidences were measured in the second half of the 82 μs window (delayed coincidence method). The correction of $-0.81(15)\%$ due to accidental coincidences was obtained directly from measured data.

The fit regions to evaluate the Q spectra were chosen according to the detailed analysis of the neutrino asymmetry parameters [9,10] generated from same (Q^{++}, Q^{--}) and opposite hemisphere (Q^{+-}, Q^{-+}) spectra. Because of the finite neutron beam width, some particles were emitted towards an increasing magnetic field and could be reflected (depending on their emission angle). For Q^{++} and Q^{--}, this "magnetic mirror" effect increases for large energies E. Thus, a smaller fit region was used. The electron detector efficiencies were verified by analyzing the trigger functions and found to be 1 above 200 keV. The proton asymmetry parameter itself varies slightly ($\pm 0.8\sigma_{\text{stat}}$) with different fit regions and their combinations, leading to an additional uncertainty of 0.35%.

At low energies, there is some HV related background left in the spectra (Fig. 1). In the fit regions, however, they can be well described by fits with a normalizing factor as the only free parameter, indicating that almost no background is left in this region. The remaining uncertainty of 0.18% was determined by using the residuals of the fits. Backscattered electrons assigned to the wrong detector also distort the spectra below 240 keV. At higher energies, backscattering leads to completely negligible corrections in the order of 0.01% [13].

Corrections associated with the design of the spectrometer, "mirror effect," "edge effect," and "grid effect," are described in [9]. They were determined by Monte Carlo simulations. For the fit regions of this analysis, all associated errors and corrections to C are small. The same holds for the influence of the coefficients $A = -0.1173(13)$, $B = 0.981(4)$, and $a = -0.103(4)$ [14] entering via Eq. (6).

Figure 1 shows the fits and integrals for one detector yielding the result

$$C = -0.2377(10)_{\text{stat}}(24)_{\text{syst}} = -0.2377(26). \quad (7)$$

A detailed summary of all corrections and uncertainties can be found in Table I. The second proton detector had a much worse proton efficiency due to an inferior carbon foil quality, leading to $C_2 = -0.245(9)$ with a more than 3 times larger uncertainty. Therefore, we only consider the precise value here, C_2 serves as cross check: Both values agree within their uncertainties. We also do not consider the result of the earlier measurement [7] with PERKEO II due to its larger systematic uncertainties.

Our final result for the proton asymmetry parameter, Eq. (7), has an uncertainty of only 1.1%. Note that it is correlated with the recently published neutrino asymmetry parameter B [9] as the analyses use partly the same data (Q^{++}, Q^{--}). Our result agrees with $C_{\text{SM}} = -0.2392(4)$, the SM expectation calculated using Eq. (3), and the world mean value $\lambda = -1.2695(29)$ [14]. It also fulfills relation

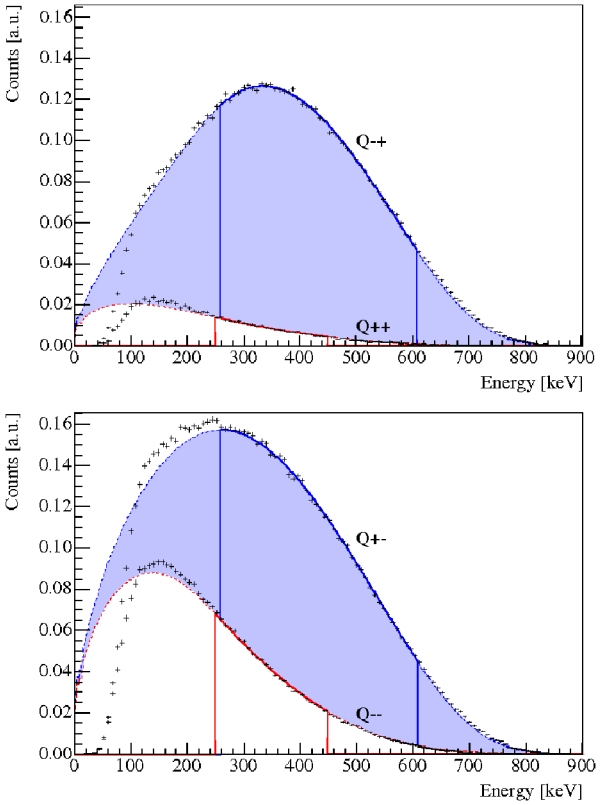

FIG. 1 (color online). The spectra to determine C from proton detector 2 were fitted in the regions indicated by the solid lines. The functions were extrapolated to cover the whole energy range and finally integrated (solid areas). The one parameter fits describe the spectra very well for $E \geq 240$ keV. The agreement between fit and data in the low energy regime can be improved by including the detector threshold and a backscattering correction to the theoretical description. We refrain from this approach since the uncorrected Q spectra, as shown in this figure, are needed to determine C. Since the magnetic mirror effect (cf. text and [9]) acts differently on Q^{ii} and Q^{ij}, $i \neq j$, the fits were performed in unequal energy regions.

(2), but the precision of C has to be improved for stringent SM cross checks. If, for example, the experimental precision of C could be improved by a factor of 3, limits on scalar- or tensorlike interactions would improve by about 20% (assuming the present values for A, B, a, and the lifetime τ_n). For the first time, the proton asymmetry can now be included in these analyses (see, e.g., [2]) to get constraints on various models beyond the SM [15]. Additionally, we can use Eq. (3) to derive the SM parameter $\lambda_{(\text{int})} = -1.282(21)$ from the *integral* proton asymmetry C, Eq. (7).

A more sensitive and direct determination of λ from the same data can be performed by a *differential* analysis of the electron energy E dependent proton asymmetry

$$C_{\text{exp}}(E) = \frac{(Q^{++} + Q^{-+}) - (Q^{+-} + Q^{--})}{(Q^{++} + Q^{-+}) + (Q^{+-} + Q^{--})}. \quad (8)$$

TABLE I. Corrections and errors of the proton asymmetry parameter C. The extrapolation uncertainty contributes to the statistical and the detector calibration errors.

Effect [%]	Correction	Error
Polarization	0.30	0.10
Flip efficiency		0.10
Data set: *Statistics*		0.44
Fit region		0.35
Accidental coincidences	−0.81	0.15
Background		0.18
Detector: *Gain*		0.38
Offset		0.82
Resolution		0.12
Spectrometer: *Mirror effect*	0.01	0.06
Edge effect	0.26	0.05
Grid effect	0.08	0.05
Correlations: A, B, a		0.07
Sum	−0.16	1.11

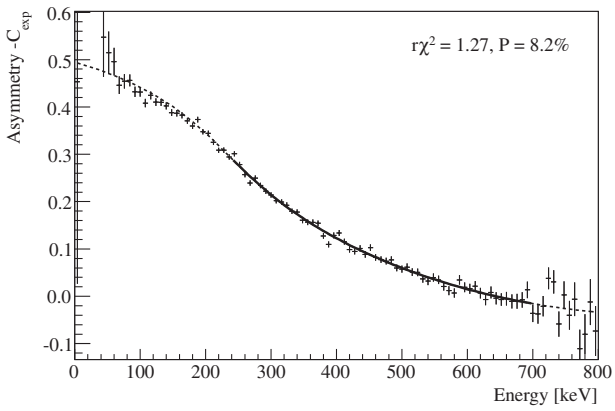

FIG. 2. The (negative) experimental proton asymmetry $-C_{\mathrm{exp}}(E)$ of proton detector 2 and the fit in order to obtain λ. Since some systematic effects cancel in the asymmetry, it can be described very well over a large energy range. The bold line indicates the fit region.

The E dependencies of the Q^{ij} have been omitted here. The fit function is calculated using Eq. (6) and replacing the coefficients a, A, and B by their SM expressions in terms of λ (as given in, e.g., [5]). In order to avoid systematic effects due to different proton efficiencies, we again use always the same hemisphere for proton detection and flip the spin. Consequently, the asymmetry (8) contains data from different electron detectors with different calibration uncertainties. In order to estimate the related systematic effects on λ, we consider the properties of the inferior detector. Again, this uncertainty dominates the overall error budget.

On the other hand, systematic effects such as the detector threshold and the magnetic mirror effect cancel in the asymmetry spectrum (8) allowing us to describe the data over a large energy region (Fig. 2): We can extend the fit region to up to 700 keV. The lower border is again 240 keV to avoid systematic effects due to different electron detector thresholds or backscattering. The result

$$\lambda_{(\mathrm{diff})} = -1.275(6)_{\mathrm{stat}}(15)_{\mathrm{syst}} = -1.275(16) \qquad (9)$$

does not depend on the fit region. Results for fits in different regions agree within $0.2\sigma_{\mathrm{stat}}$. The overall uncertainty of 1.2% is dominated by detector calibration (gain 0.68%, offset 0.82%) and statistics (0.50%). All other uncertainties are much smaller. $\lambda_{(\mathrm{diff})}$ agrees with $\lambda_{(\mathrm{int})}$ derived from the integral proton asymmetry which is an important cross check for the integration and extrapolation procedure.

We recommend the value $\lambda_{(\mathrm{diff})}$, Eq. (9), as a result for λ from our experiment as it is more precise and more direct than $\lambda_{(\mathrm{int})}$. It agrees well with the world mean value derived from measurements of the beta asymmetry A. It is almost 1 order of magnitude less precise but has been obtained using a new method with different systematics. A proton asymmetry precision of better than 0.1% would yield a stringent contribution to λ determinations obtained so far from electron asymmetry A measurements (for an overview, cf. [1]). This precision, however, can presumably only be achieved with next generation instruments.

We thank D. Dubbers for his support in all phases of the experiment. We thank the summer students A. Hillairet, T. Moschoutis, and S. Schnez. Work was funded by the German Federal Ministry for Research and Education, Contracts No. 06HD153I, No. 06HD187.

*marc.schumann@gmx.net
†Present address: Institut Laue-Langevin, Grenoble
‡abele@e18.physik.tu-muenchen.de

[1] H. Abele, Prog. Part. Nucl. Phys. **60**, 1 (2008).
[2] N. Severijns, M. Beck, and O. Naviliat-Cuncic, Rev. Mod. Phys. **78**, 991 (2006).
[3] S. B. Treiman, Phys. Rev. **110**, 448 (1958).
[4] F. Glück, Phys. Lett. B **376**, 25 (1996).
[5] F. Glück, I. Joó, and J. Last, Nucl. Phys. **A593**, 125 (1995).
[6] S. K. L. Sjue, Phys. Rev. C **72**, 045501 (2005).
[7] M. Kreuz, Ph.D. thesis, University of Heidelberg, 2004, www.ub.uni-heidelberg.de/archiv/4799/.
[8] H. Abele *et al.*, Nucl. Instrum. Methods Phys. Res., Sect. A **562**, 407 (2006).
[9] M. Schumann *et al.*, Phys. Rev. Lett. **99**, 191803 (2007).
[10] M. Schumann, Ph.D. thesis, University of Heidelberg, 2007, www.ub.uni-heidelberg.de/archiv/7357.
[11] M. Kreuz *et al.*, Nucl. Instrum. Methods Phys. Res., Sect. A **547**, 583 (2005).
[12] M. Kreuz *et al.*, Phys. Lett. B **619**, 263 (2005).
[13] M. Schumann and H. Abele, Nucl. Instrum. Methods Phys. Res., Sect. A **585**, 88 (2008).
[14] W.-M. Yao *et al.* (PDG), J. Phys. G **33**, 1 (2006).
[15] P. Herczeg, Prog. Part. Nucl. Phys. **46**, 413 (2001).